

## Supplementary Information for Biodegradable Nanoparticles Aid the Gut Microbial Community in Delaying Antibiotic Resistance Emergence

**Genesis Herrera<sup>1</sup>, Sachin Paudel<sup>2</sup>, Simone Lupini<sup>3</sup>, Carlos Astete<sup>4</sup>, Cristina Sabliov<sup>5</sup>, Debora Rodrigues<sup>6</sup>**

<sup>1</sup>Graduate Student, Dept. of Biology and Biochemistry, University of Houston, Houston, TX, 77004, e-mail: [gherre21@cougarnet.uh.edu](mailto:gherre21@cougarnet.uh.edu)

<sup>2</sup>Graduate, Dept. of Civil and Environmental Engineering, University of Houston, Houston, TX, 77004, email: [Sachin.paudel@gmail.com](mailto:Sachin.paudel@gmail.com)

<sup>3</sup>Graduate Student, Dept. of Biology and Biochemistry, University of Houston, Houston, TX, 77004, e-mail: [slupini@central.uh.edu](mailto:slupini@central.uh.edu)

<sup>4</sup>Professor, Dept. of Biological & Agricultural Engineering, Louisiana State University, Baton Rouge, LA, 70803, e-mail: [castete@agcenter.lsu.edu](mailto:castete@agcenter.lsu.edu)

<sup>5</sup>Professor, Dept. of Biological & Agricultural Engineering, Louisiana State University, Baton Rouge, LA, 70803, e-mail: [CSabliov@agcenter.lsu.edu](mailto:CSabliov@agcenter.lsu.edu)

<sup>6</sup>Professor, Dept. of Civil and Environmental Engineering, University of Houston, Houston, TX, 77004, e-mail: [dfrigiuro@central.uh.edu](mailto:dfrigiuro@central.uh.edu)

### **This file includes:**

Materials and Methods  
Tables S1 to S2  
Figures S1 to S7  
SI References

## Materials and Methods

### MinION Mk1C 16S Barcoding Kit 1-24 (SQK-16S024) Sequencing

Polymerase chain reactions (PCR) for each cDNA sample (6 conditions with three-time points for a total of 18 samples) were amplified and ligated with a unique barcode on the full-length 16S rRNA region following the protocol described in the 16S Barcoding Kit 1-24 (SQK-16S024) (Oxford Nanopore Technologies (ONT)). The forward primer used was 5' ATCGCCTACCGTGAC-barcode-AGAGTTTGATCMTGGCTCAG 3', and the reverse primer was 5' ATCGCCTACCGTGAC-barcode-CGGTTACCTTGTTACGACTT 3'. Each sample cDNA concentration was diluted to 1 ng/ $\mu$ L. The 50  $\mu$ L PCR reaction contained 10  $\mu$ L of cDNA template, 25  $\mu$ L of LongAmp Taq 2X Master Mix (New England Biolabs, USA), 10  $\mu$ L of specific barcode, and 5  $\mu$ L of nuclease-free water. The thermal cycling conditions were: 95 °C for 1 min, denaturation for 25 cycles at 95 °C for 20 s, annealing at 55 °C for 30 s, extension at 65 °C for 2 min, and a final extension at 65 °C for 5 min. The PCR products were cleaned following the kit protocol using a magnetic rack and AMPure XP beads (Beckman Coulter, USA) and eluted in 10  $\mu$ L of 10 mM Tris-HCl pH 8.0 with 50 mM NaCl. Each sample library was quantified using a Take 3 micro-volume plate reader (BioTek Synergy) to pool the library into equal concentration ratios. The flow cell was primed before loading the barcoded samples in the kit per the protocol. An aliquot of 75  $\mu$ L of the pooled libraries was loaded in the R9.4.1 flow cell on the ONT MinION Mk1C device (ONT, London, UK). After basecalling the reads were filtered by length and quality, the average number of reads per condition was 2,190. The average read length was 2,706 base pairs. These metrics reflect the impact of our length filtering strategy, resulting in fewer but longer reads. Raw sequencing reads quality were determined Oxford Nanopore Technologies EPI2ME software for quality control. The average quality score of the reads was 11.58.

### DNA Extraction and 16S rRNA Metagenomic Sequencing

After 48 hours of incubation three technical replicates of the pig slurry in the anaerobic bioreactor, 15 mL of the slurry was collected for DNA extractions. According to the manufacturer's protocol, the DNA extractions were conducted with the Quick-DNA Fungal/Bacterial Miniprep kit (Zymo Research, Irvine, CA, USA). The sample was stored at -20 °C overnight and then extracted for DNA. Once removed, the DNA was immediately analyzed. An Agilent BioTek bioanalyzer and a Qubit Broad Range DNA assay were used to determine the purity and integrity of the extracted DNA. The same protocol as the ONT 16S rRNA barcoding kit for sequencing was used.

### MinION Mk1C Rapid Barcoding Kit 96 (SQK-RBK110.96) Resistome Sequencing

Polymerase chain reaction (PCR) of each cDNA sample (6 conditions at 72 h for a total of 6 samples) was ligated with a unique barcode on total cDNA following Barcoding Kit 96 (SQK-RBK110.96) (Oxford Nanopore Technologies (ONT)). For each sample, the 10  $\mu$ L PCR reaction contained 9  $\mu$ L of 50 ng template DNA and 1  $\mu$ L Rapid Barcodes (RB01-96, one for each sample). The thermal cycling conditions were 30°C for 2 min, then 80°C for 2 min. The PCR products were cleaned following the kit's protocol using a magnetic rack and eluted in 10  $\mu$ L of 10 mM Tris-HCl pH 8.0 with 50 mM NaCl. Each sample library was quantified using an Invitrogen Qubit Fluorometer to pool the library into equal concentration ratios. An aliquot of 75  $\mu$ L of the pooled libraries was loaded in the R9.4.1 flow cell on the ONT MinION Mk1C device

(ONT, London, UK). The flow cell was primed before loading the barcoded samples per the kit's manufacturer's protocol. After basecalling the reads were filtered by length and quality, the average number of reads per condition was 7132. The average read length was 545 base pairs. Raw sequencing reads quality were determined using Oxford Nanopore Technologies EPI2ME software for quality control. The average quality score of the reads was 10.25.”

### **Statistical Analysis**

The statistical significance difference between the samples, reported as a p-value, was calculated using a one-way analysis of variance (ANOVA), t-test, and F-test statistics from the MicrobiomeAnalyst.(1-3) The Bray Curtis index was used to determine the  $\beta$  (beta) diversity.(4) The presence of a difference between the centroid values across the various samples was evaluated through a permutational multivariate analysis of variance (PERMANOVA) using the function *adonis2*, built into the *vegan* package.(5) Non-metric Multidimensional Scaling (NMDS)(6) was executed using the *vegan* package in R Studio.(7) The statistic test, F-test, and coefficient of determination (R-squared) were used to determine the p-value for the non-metric multidimensional scaling (NMDS).(8) The genus-level relative abundance was used to create a clustered heatmap based on Pearson distance measurement and Ward clustering algorithm using MicrobiomeAnalyst.(3, 8) Statistical analysis was performed using Excel (Microsoft Corporation, Redmond, WA, United States), R Studio, and Origin (OriginLab Corporation, Northampton, MA, United States). The network analysis was performed using the R package *igraph*.(9) Furthermore, the statistical significance presented in **Figure 4** was determined using the Adonis analysis with an Euclidean method (1000 permutations, nanoparticle: antibiotic  $R^2= 0.45349$ ; F-value= 3.2116).

## Supporting Figures

**Table S1.** Composition Nutritive Media to Culture Swine Gut Microbiome

The nutritive media emulating the small intestine culture environment for the bacterial community for the swine's small intestinal slurry was prepared based on literature with a few modifications.(10-12)

<b>Ingredient</b>	<b>g/L</b>
Corn Starch	11.32
Pectin (apple)	4.32
Xylan (Beechwood)	2.00
Arabinogalactan (larch wood)	2.00
Guar Gum	2.00
Soy Peptone	13.00
Yeast Extract	4.50
Mucin (from porcine stomach	4.00
L-cysteine HCl monohydrate	0.80
Bile extract from porcine	0.40
KH <sub>2</sub> PO <sub>4</sub>	0.50
NaHCO <sub>3</sub>	1.50
NaCl	4.50
KCl	4.50
MgSO <sub>4</sub> anhy. (120.37 g/mol)	0.64
CaCl <sub>2</sub> . 2H <sub>2</sub> O (147.02 g/mol)	0.15
MnCl <sub>2</sub> . 4H <sub>2</sub> O (197.91 g/mol)	0.20
Tween 80	1.00

**Table S2.** Antibiotic Class and Their Mechanism of Action

<b>Antibiotic Class</b>	<b>Mechanism of Action</b>
Aminoglycoside	Bind to 30S/50S bacterial ribosomal subunit to inhibit peptidyl-tRNA translocation, causing mRNA misread; accordingly, the bacteria cannot synthesize proteins.(13)
Tetracycline	Bind to 30S bacterial ribosomal subunit to inhibit aminoacyl-tRNA binding to the mRNA-ribosome complex.(13)
Lincomycin	Inhibit the peptidyl transferase reaction on the 50S bacterial ribosomal subunit, blocking protein synthesis.(14)
Elfamycin	The elongation factor Tu (EF-Tu) is a nucleotide-binding protein essential for protein synthesis. An elfamycin mechanism is a group of structurally diverse antibiotics that impair the function of EF-Tu during the translation of protein synthesis.(15)
Fluoroquinolone	Inhibit the bacterial DNA gyrase or topoisomerase IV enzyme inhibits DNA replication and transcription.(13)

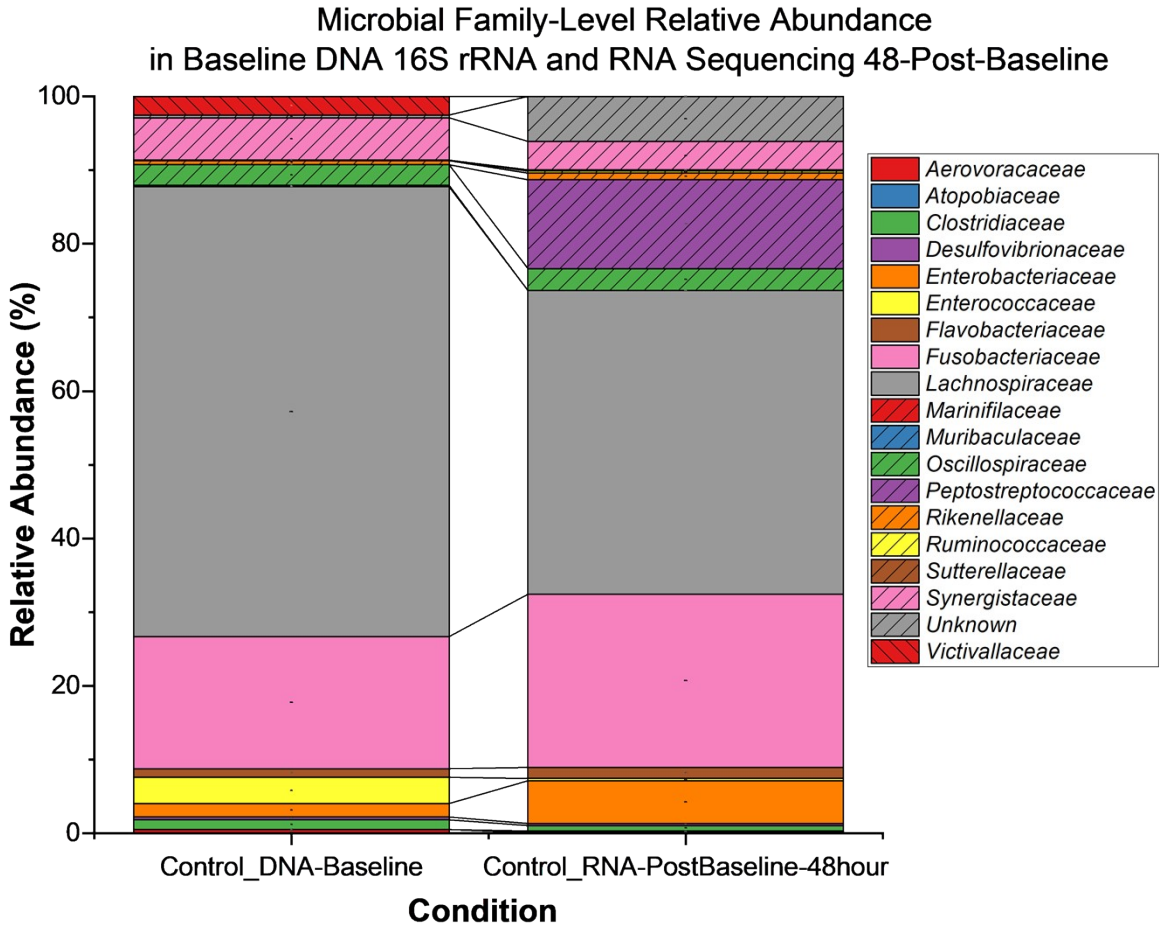


**Figure S1.** Microbial relative abundance at family level in DNA 16S rRNA sequencing after steady state reached by the microbial community and RNA sequencing of the control group post-treatment containing similar microbial families. The relative abundance of microbial families after 48 hours of DNA 16S rRNA sequencing shows the baseline. The control group's abundance, measured 48 hours after the baseline using RNA sequencing, is also displayed.

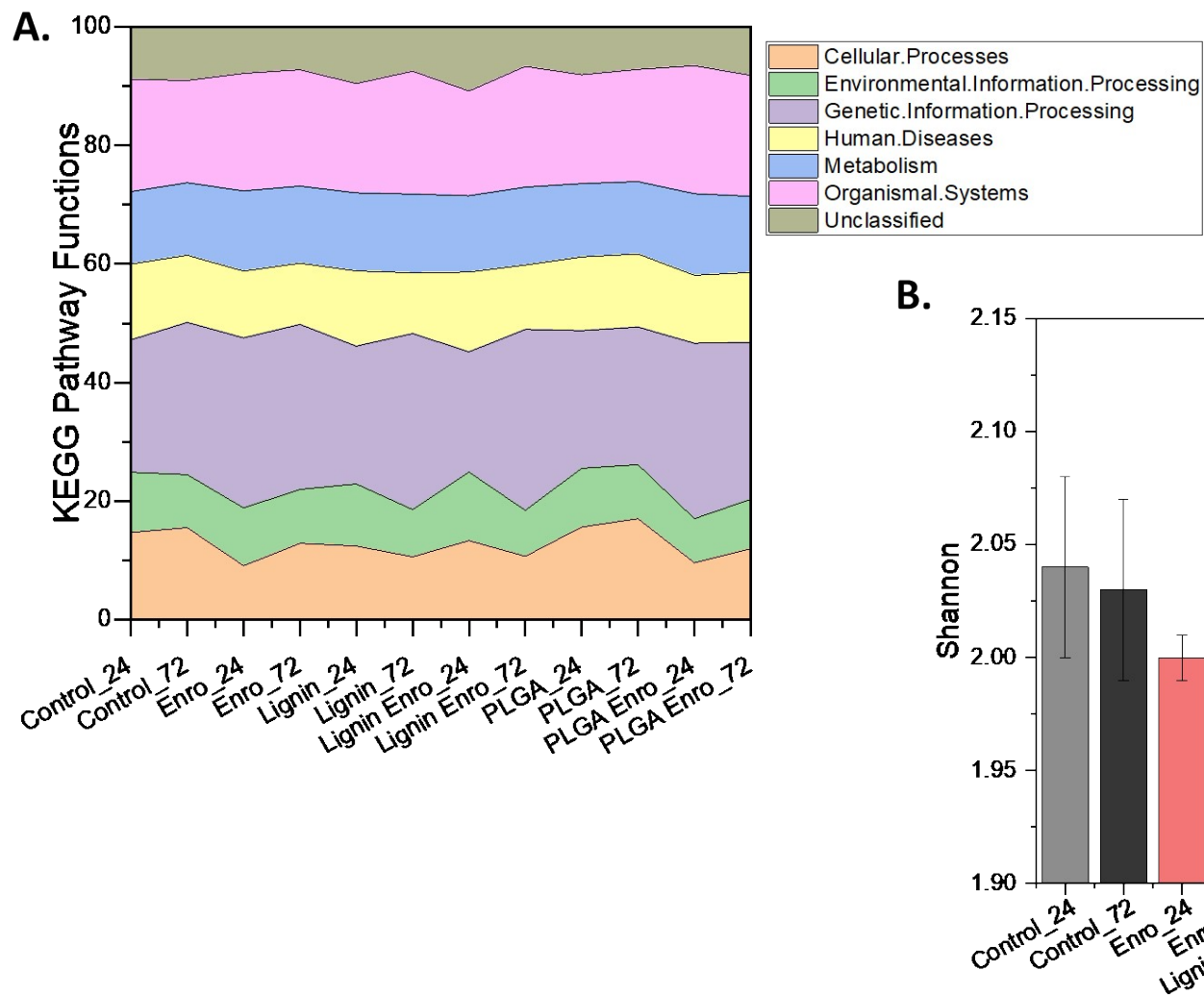


**Figure S2.** Metabolic function analysis and alpha diversity estimation: comparing conditions at 24- and 72-h post-treatment using PICRUST analysis of 16S rRNA. A) Stacked bar plot on the various metabolic functions estimated by PICRUST using the 16S rRNA fastq files for each condition during 24 and 72 h post treatment that corroborates 16S microbial community shifts findings. B) Alpha diversity bar chart: P-value = 0.129 from a one-way ANOVA F-value = 1.914 determined from the estimated 16S microbial functions.

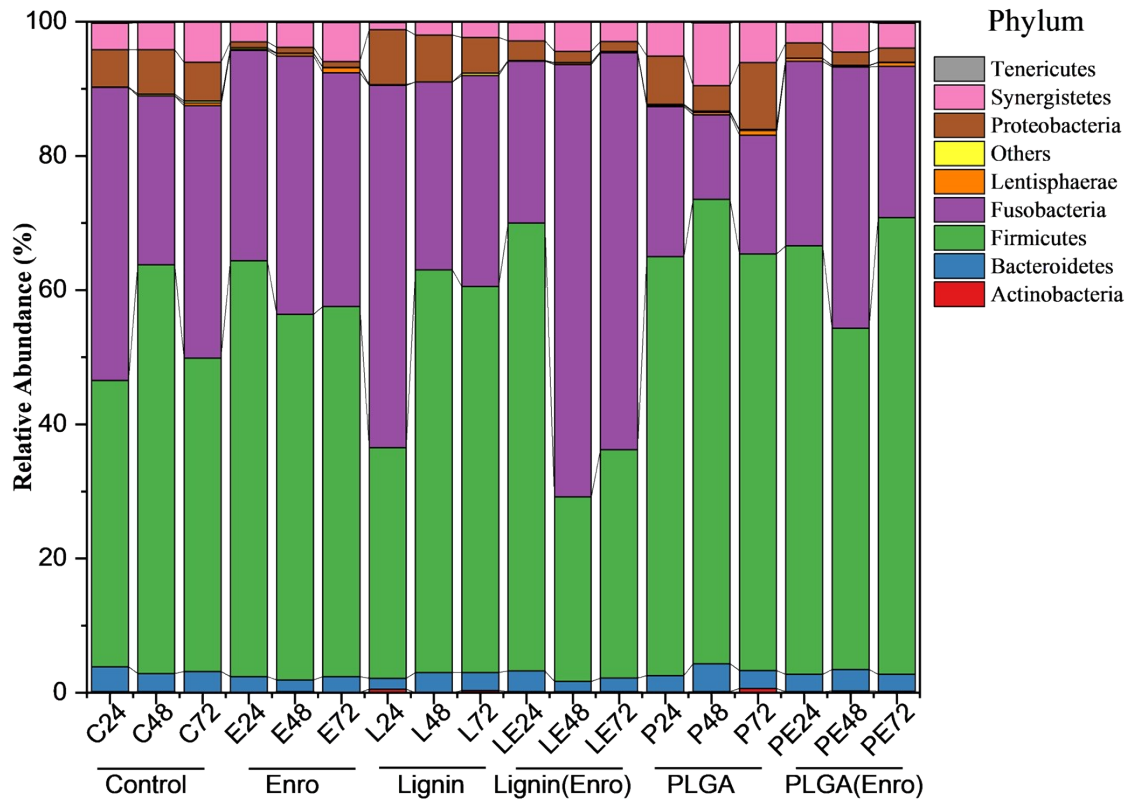


**Figure S3.** Relative abundance of dominant gut microbial systems at the phylum level.



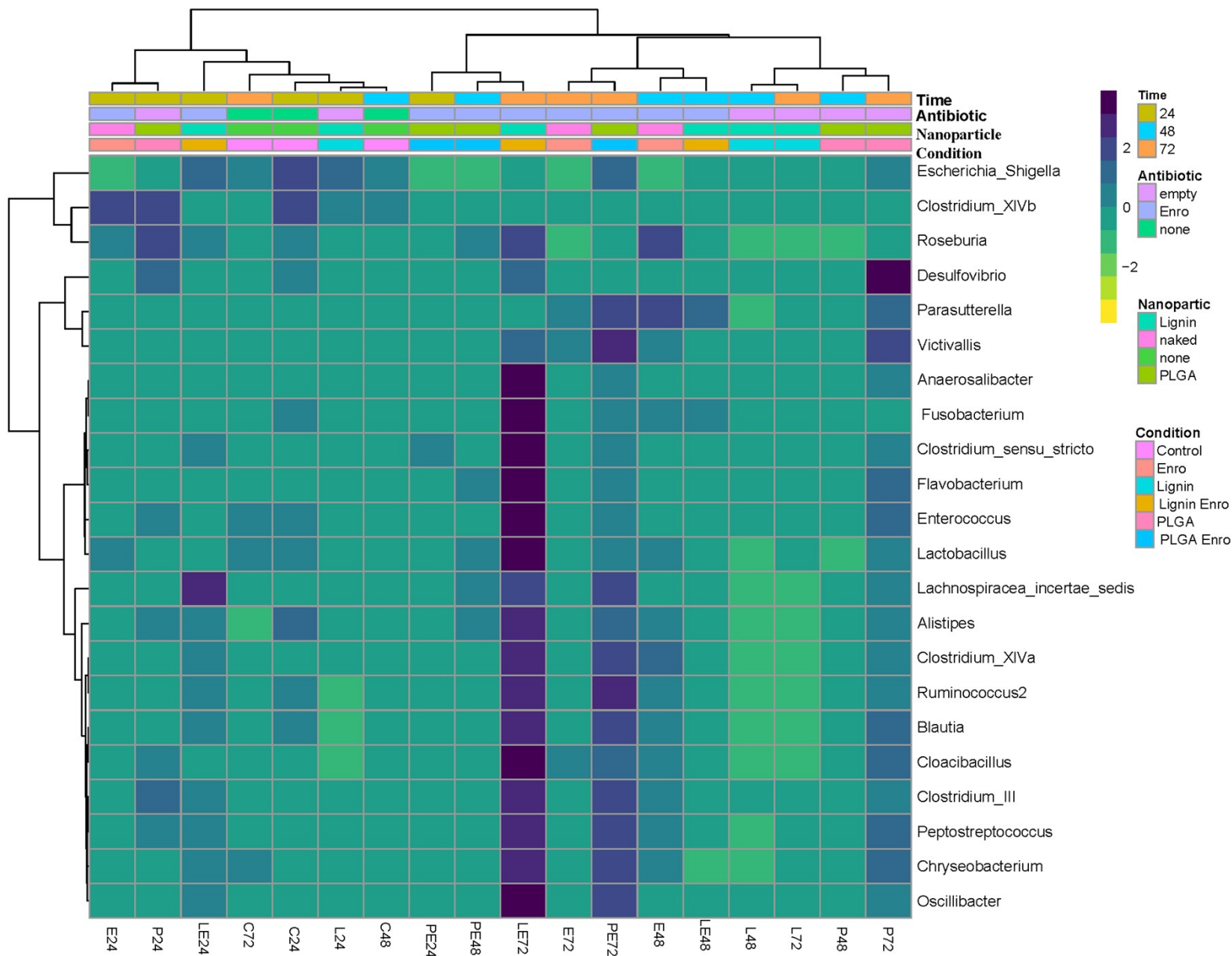


**Figure S4.** Clustered heatmap on the relative abundance of organisms at the genus level for each sample with information on the condition, nanoparticle type, and presence of an antibiotic. The clustered heatmap was created using the Pearson distance measure, the Ward clustering algorithm, and the condition's experimental factor.

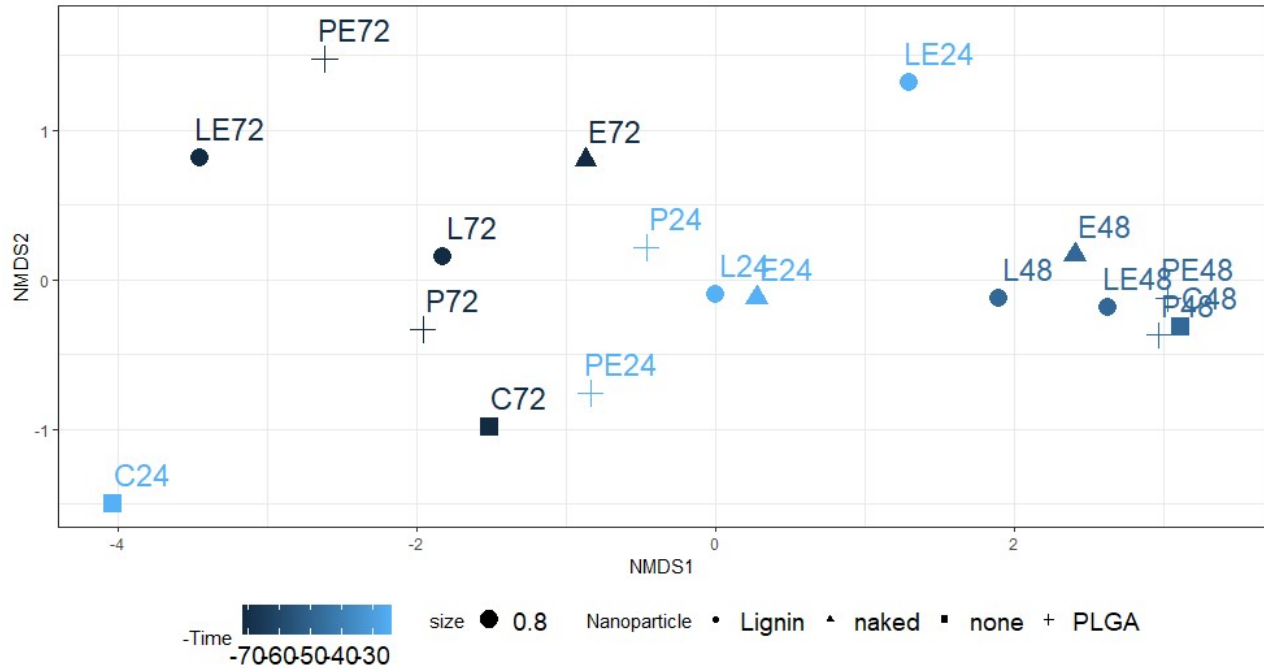


**Figure S5.** NMDS plot shows the relationship of ARGs of each condition for all treatment periods; naked is free Enrofloxacin, and none indicates control with no treatment. We found no statistical significance between nanoparticles and antibiotics (p-value = 0.932).

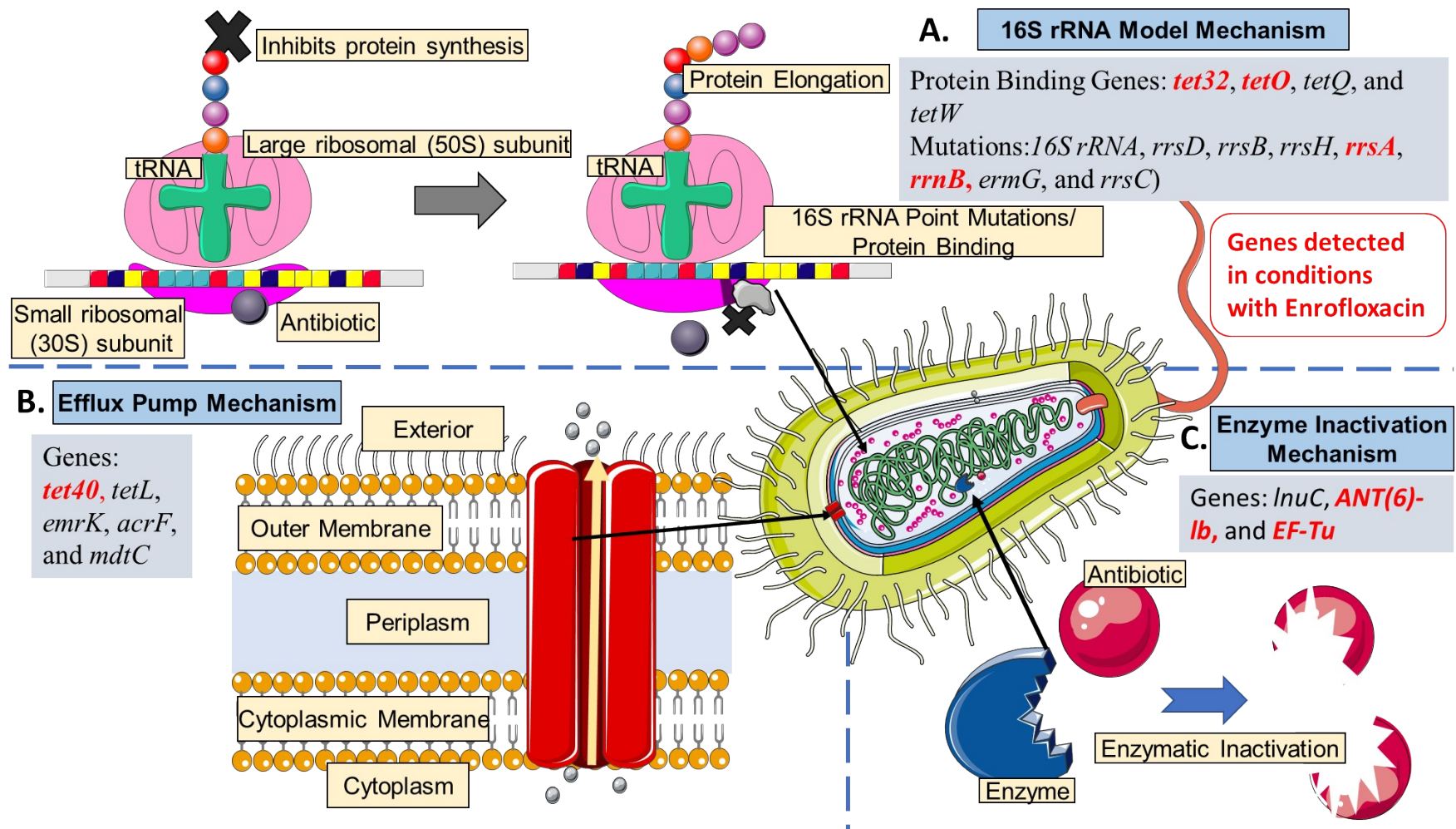


**Figure S6.** Antibiotic resistance mechanisms overview and genes in red were observed with free enrofloxacin or loaded NPs. A) 16S rRNA Model: 16S rRNA methylation/point mutations interrupt antibiotic and 30S ribosomal subunit affinity, allowing translation to proceed.(16) B) Efflux Pump: transport protein that extrudes antibiotics from cytoplasm to the external environment.(17) C) Enzyme Inactivation: antibiotic degrading enzymes.(18) Figure created with images, markings, and annotation from Servier Medical Art by Servier, licensed under a Creative Commons Attribution 3.0 Unported License.

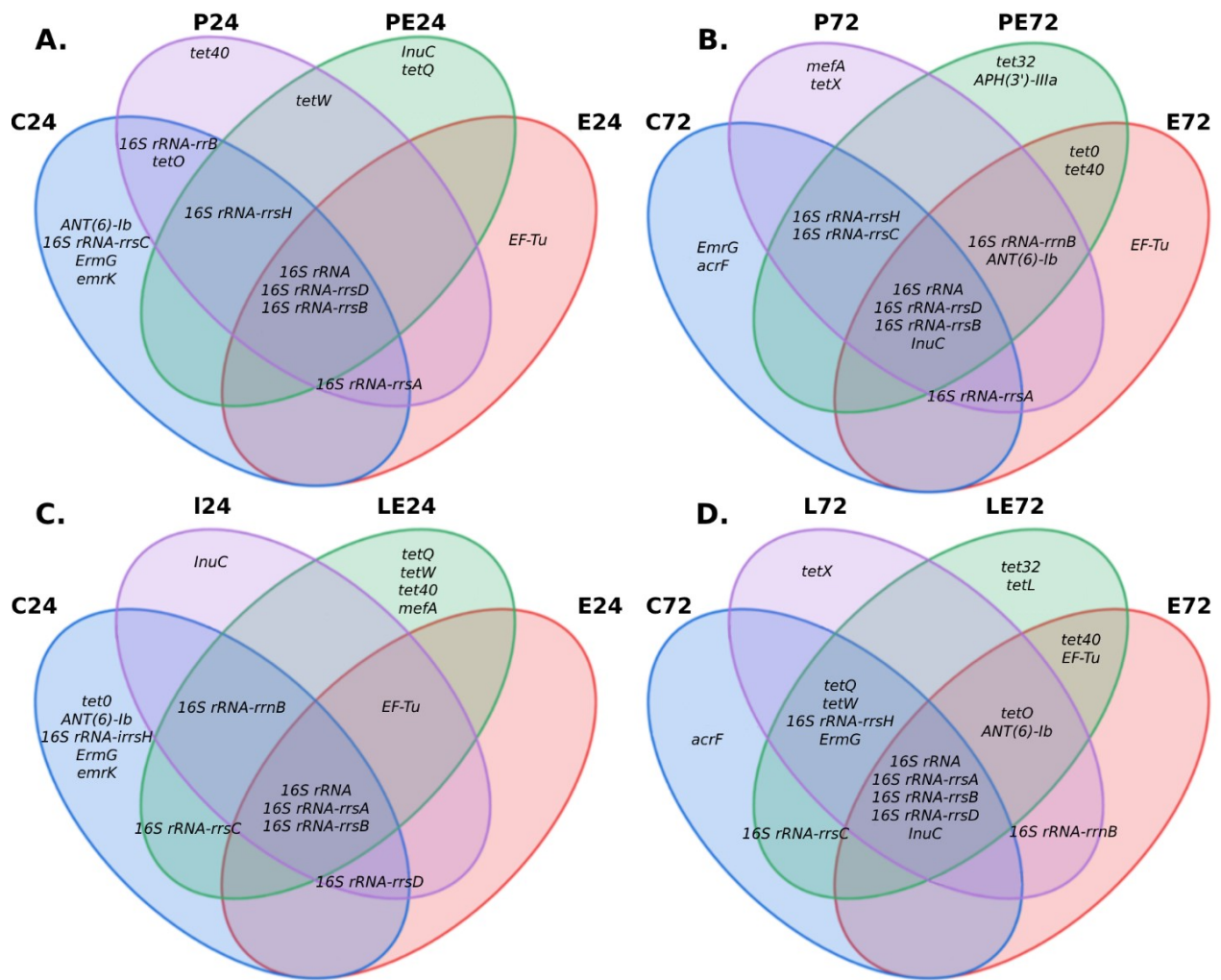


**Figure S7:** ARGs appearing in all conditions with Enrofloxacin are highlighted in the Venn diagram for both nanoparticles with respective controls (no treatment (C) and free Enrofloxacin (E)). A) PLGA empty (P24) and loaded with Enro (PE24) NPs at 24 hours. B) PLGA empty (P72) and loaded with Enro (PE72) NPs at 72 hours. C) Lignin empty (L24) and loaded with Enro (LE24) NPs at 24 hours. D) Lignin empty (L72) and loaded with Enro (LE72) NPs at 72 hours.



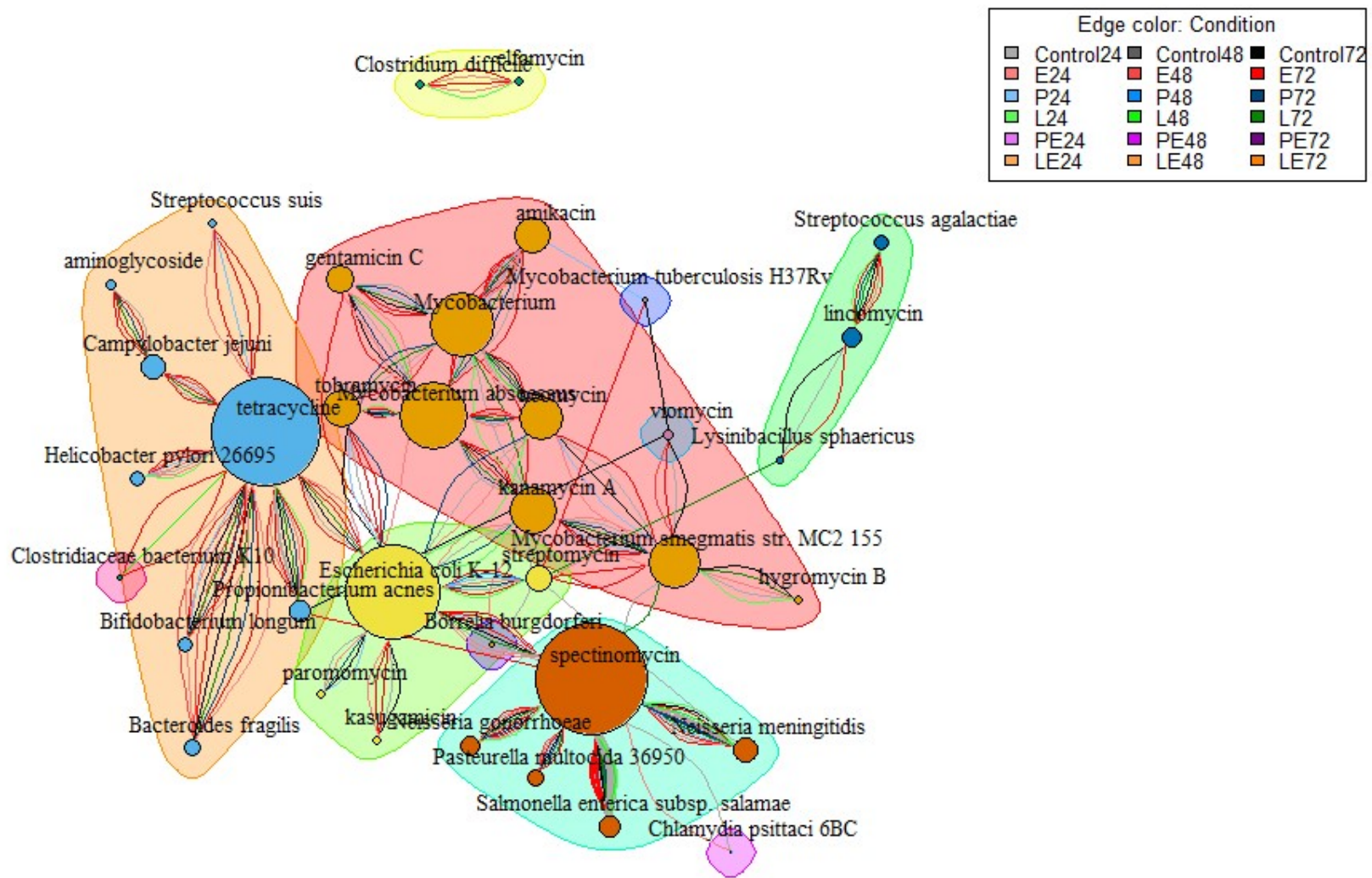


**Figure S8.** The correlation network analysis graph consists of vertices (shown as circles) representing the ARG species hosts and ARG subtypes. The vertices are connected by edges, with the thickness of the edges defining the strength of correlation between the two variables. Thicker lines indicate a stronger correlation, while thinner lines indicate a weaker correlation. The vertex size also encodes the relative importance or weight.

## Supplementary Information References

1. Kaufmann J, Schering A. Analysis of Variance ANOVA. Wiley StatsRef: Statistics Reference Online.
2. STUDENT. THE PROBABLE ERROR OF A MEAN. *Biometrika*. 1908;6(1):1-25.
3. Mann BC, Bezuidenhout JJ, Swanevelder ZH, Grobler AF. MinION 16S datasets of a commercially available microbial community enables the evaluation of DNA extractions and data analyses. *Data in Brief*. 2021;36:107036.
4. Bray JR, Curtis JT. An Ordination of the Upland Forest Communities of Southern Wisconsin. *Ecological Monographs*. 1957;27(4):325-49.
5. Anderson MJ. Permutational Multivariate Analysis of Variance (PERMANOVA). Wiley StatsRef: Statistics Reference Online. p. 1-15.
6. Kruskal JB. Nonmetric multidimensional scaling: A numerical method. *Psychometrika*. 1964;29(2):115-29.
7. Team R. RStudio: Integrated Development for R. . 2021.09.1-372 ed. Boston, MA: PBC; 2020.
8. Shetty SA, Lahti L. Microbiome data science. *Journal of Biosciences*. 2019;44(5):115.
9. Csárdi G, Nepusz T, editors. The igraph software package for complex network research2006.
10. Marcus Ian M, Wilder Hailey A, Quazi Shanin J, Walker Sharon L. Linking microbial community structure to function in representative simulated systems. *Appl Environ Microbiol*. 2013;79(8):2552-9.
11. Macfarlane GT, Macfarlane S, Gibson GR. Validation of a three-stage compound continuous culture system for investigating the effect of retention time on the ecology and metabolism of bacteria in the human colon. *Microbial Ecology*. 1998;35(2):180-7.
12. Tanner SA, Zihler Berner A, Rigozzi E, Grattepanche F, Chassard C, Lacroix C. In Vitro Continuous Fermentation Model (PolyFermS) of the Swine Proximal Colon for Simultaneous Testing on the Same Gut Microbiota. *PLOS ONE*. 2014;9(4):e94123.
13. Adzitey F. Antibiotic classes and antibiotic susceptibility of bacterial isolates from selected poultry; a mini review. 2015.
14. Spížek J, Řezanka T. Lincomycin, clindamycin and their applications. *Applied Microbiology and Biotechnology*. 2004;64(4):455-64.
15. Yarlaga V, Medina R, Johnson TA, Koteva KP, Cox G, Thaker MN, et al. Resistance-guided discovery of elfamycin antibiotic producers with antigenococcal activity. *ACS Infectious Diseases*. 2020;6(12):3163-73.
16. Guitor AK, Wright GD. Antimicrobial resistance and respiratory infections. *Chest*. 2018;154(5):1202-12.
17. Sharma A, Gupta VK, Pathania R. Efflux pump inhibitors for bacterial pathogens: From bench to bedside. *Indian J Med Res*. 2019;149(2):129-45.
18. Schaefer AJ, Wright GD. Antibiotic resistance by enzymatic modification of antibiotic targets. *Trends in Molecular Medicine*. 2020;26(8):768-82.